Journal of Geosciences, 55 (2010), 57–67 DOI: 10.3190/jgeosci.059

Original paper

Aquamarine beryl from Zealand Station, Canada: a mineralogical and stable isotope study

Kristy-Lee BEAL*, David R. LENTZ

Department of Geology, University of New Brunswick, Fredericton, New Brunswick, E3B 5A3, Canada; k.beal@unb.ca, dlentz@unb.ca
** Corresponding author*

Aquamarine crystals occur in crustal A-type pegmatite–aplite dykes and associated quartz veins and greisen zones at the Zealand Station Be–Mo deposit, south-central New Brunswick (Canada). Electron-probe microanalysis (EPMA) of aquamarine determined that the chromophore Fe (< 1.4 wt. % FeO^T) is present in octahedral sites, with substitutions responsible for simple and oscillatory zonation (SEM–BSE imaging). Average water content (1.53 wt. %) was calculated using an empirical formula, consistent with two T_{REL} (>800 °C) of 1.3–1.4 wt. % in beryl channels. The $\delta^{18}O$ of the quartz and beryl were within 1 ‰, consistent with magmatic crystallization from an ^{18}O enriched source, and δD values on channel water have magmatic signatures.

Keywords: aquamarine, pegmatite, aplite, Allandale Granite, Zealand Station, New Brunswick
Received: 16 November 2009; accepted 12 March 2010; handling editor: M. Novák

1. Introduction

Beryllium is a relatively rare element in the Earth's crust, ranking 47th most abundant. It averages approximately 3 ppm in the upper crust, which is fairly elevated compared to 60 ppb inferred in the primitive mantle (Grew 2002). Beryl, the most common beryllium-bearing mineral in the Earth's crust, occurs in granites, granite pegmatites, and in veins. Beryl can form at any stage of pegmatite consolidation/crystallization, by autometasomatic processes, and during hydrothermal events (Černý 2002; Wang et al. 2009). Beryl is a tectosilicate (Aurisicchio et al. 1988), with the ideal formula expressed as $Be_3Al_2Si_6O_{18}$, although elemental substitutions in the structure cause the formula to become more complex (Černý 2002). Beryl has a hexagonal structure where the six-member rings of Si-bearing tetrahedra (SiO_4) are stacked in the c-direction and linked laterally with a relative rotation of 30° between adjacent rings. These rings are linked in the direction of the a-axis by Be-bearing tetrahedra (BeO_4) and together they stack in the c-axis. Al-bearing octahedra (*O*) provide further linkages parallel and perpendicular to the c-axis (Hawthorne and Humincki 2002; Černý et al. 2003). With all the substitutions considered within the beryl structure, the formula becomes $^{C}(Na,Cs)_{2X-Y+Z}\ ^{C}(H_2O,He,Ar)_{\leq 2-(2X-Y+Z)+Na}\ ^{T(2)}(Be_{3-X}Li_Y\square_{X-Y})\ ^{O}(Al,Fe,Sc,Cr,V)_{2-Z}\ ^{O}(Fe,Mg,Mn)^{2+}_{Z}\ ^{T(1)}Si_6O_{18}$, where $Y \leq 2$, $X \geq Y$, $Z \ll 2$ and $2X-Y+Z \leq 2$ (Černý 2002; Diego Gatta et al. 2006); C are the channel sites. The substitutions cause distortion in the beryl structure, as well as variation in the bond-length and bond-angles (Aurisicchio et al. 1988).

There are several aquamarine deposits in Canada; the most notable among them is the True Blue aquamarine showing in the Yukon Territory (Turner et al. 2007). There are currently fourteen known beryl occurrences in New Brunswick that are hosted in a number of different environments related to differentiated felsic magmas (Fig. 1). The Zealand Station Be–Mo deposit, initially staked in the early 1950s because of a molybdenite occurrence, is located approximately 25 km northwest of Fredericton. The aquamarine crystals at the Zealand Station deposit attain up to 8 cm in diameter and are of clear to milky, light to medium blue colour and commonly euhedral to subhedral. The compositions of the beryl grains were studied to classify the origin of the pegmatite and the nature of the related hydrothermal fluids.

2. Geological setting

The Zealand Station aquamarine deposit is located along the northeastern cusp of the Early Devonian Hawkshaw Granite of the Pokiok Batholith. The Hawkshaw Granite intruded the metasedimentary rocks of the Silurian Kingsclear Group (Caron 1996). The Pokiok Batholith consists of five units, from oldest to youngest: Hartfield Tonalite dated at 415 ± 1 Ma (U-Pb titanite), Hawkshaw Granite (411 ± 1 Ma, U-Pb titanite), Skiff Lake Granite (409 ± 2 Ma, U-Pb zircon), Lake George Granodiorite Stock (412 +5/–4 Ma, U-Pb zircon), and Allandale Granite, which was dated at 402 ± 1 Ma by U-Pb monazite (Whalen 1993; Whalen et al. 1996). The Pokiok Batholith is the result of the Acadian Orogeny, which is noted

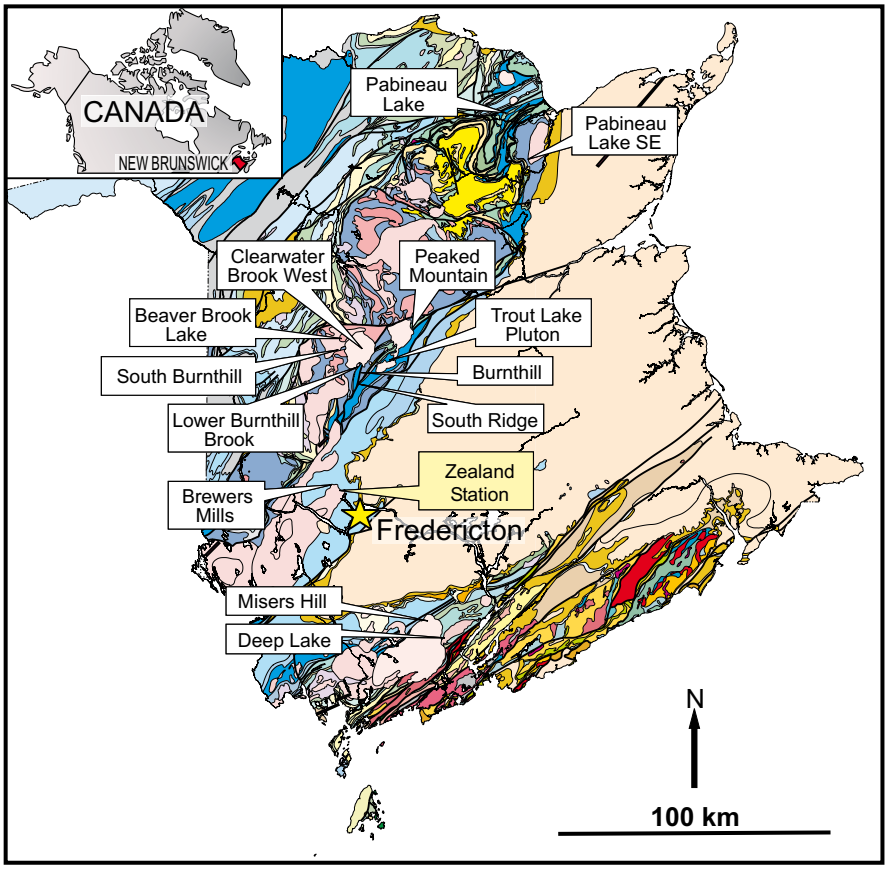

Fig. 1 Geologic map of New Brunswick showing the locations of all known beryl occurrences (DNR-NB bedrock map NR-1 2005, see *http://www.gnb.ca/0078/minerals/PDF/Bedrock_Geology_MapNR1-e.pdf* for map unit descriptions).

for associated syn- to post-tectonic granitoid intrusions from 410 to 380 Ma (Rast and Skehan 1993). This area of New Brunswick is situated in the Central Mobile Belt of the Canadian Appalachian Orogen and is viewed as a result of evolving geological environments involving the opening and closure of the Precambrian–Early Paleozoic Iapetus Ocean (Whalen et al. 1996).

The Zealand Station aquamarine deposit is hosted within an aquamarine-rich section of a SE-trending pegmatite–aplite dyke and in association with hydrothermal features including quartz veins and greisen zones in the host monzogranite, inferred to be the Hawkshaw Granite. This fine- to coarse-grained monzogranite is subdivided into three different facies based on field observations by Chrzanowski and Elliott (1986): (1) pink granite, (2) white granite, and (3) biotite-rich granite (Fig. 2). The petrological and geochemical differences between the individual intrusive phases are insignificant and all exhibit gradational contacts over 0.5 m to 1 m. All sub-types of the host monzogranite contain quartz, feldspars, biotite, rutile, and muscovite with trace zircon, monazite, and xenotime.

The SE-trending pegmatite–aplite dykes crosscut the host monzogranite and contain an aquamarine-bearing section in the largest dyke that is approximately 50 m by 2 m (Fig. 2). The dykes are locally porphyritic with euhedral quartz (up to 4 cm) and orthoclase (up to 15 cm) phenocrysts and contain additional quartz, orthoclase, albite, primary muscovite, trace to local 5 % biotite and accessory monazite, zircon, apatite, wolframite, and xenotime in the aplitic groundmass. This particular dyke has been dated at 400.5 ± 1.2 Ma using U-Pb TIMS on magmatic zircon linking this phase to the Allandale Granite of the Pokiok Batholith (Beal et al. 2010). The aquamarine-bearing section (Fig. 3a) contains approximately 30 to 40 % of blue aquamarine crystals (<2 cm wide), albite, orthoclase, primary muscovite, and minor quartz with accessory rutile, calcite, monazite, zircon, apatite, and xenotime (Fig. 3b). The contacts of the aquamarine-bearing section with the dyke are sharp and marked locally by abundant biotite. This aquamarine-bearing section was dated at 404 ± 8 Ma (U-Th-Pb monazite; Beal et al. 2010) linking the mineralization to the dyke.

There is a 2 m by 2 m pegmatite outcrop located approximately 50 m east of the mapped area and consists of a border zone, intermediate zone, and a core of predominately plagioclase and quartz up to 15 cm, biotite booklets up to 3 cm wide, and wolframite crystals up to 3 cm long. The border and intermediate zones contain orthoclase, albite, quartz, and primary muscovite with trace amounts of biotite, zircon, rutile, monazite, chlorite, calcite, and iron-oxides. No beryl has been identified in this pegmatitic phase.

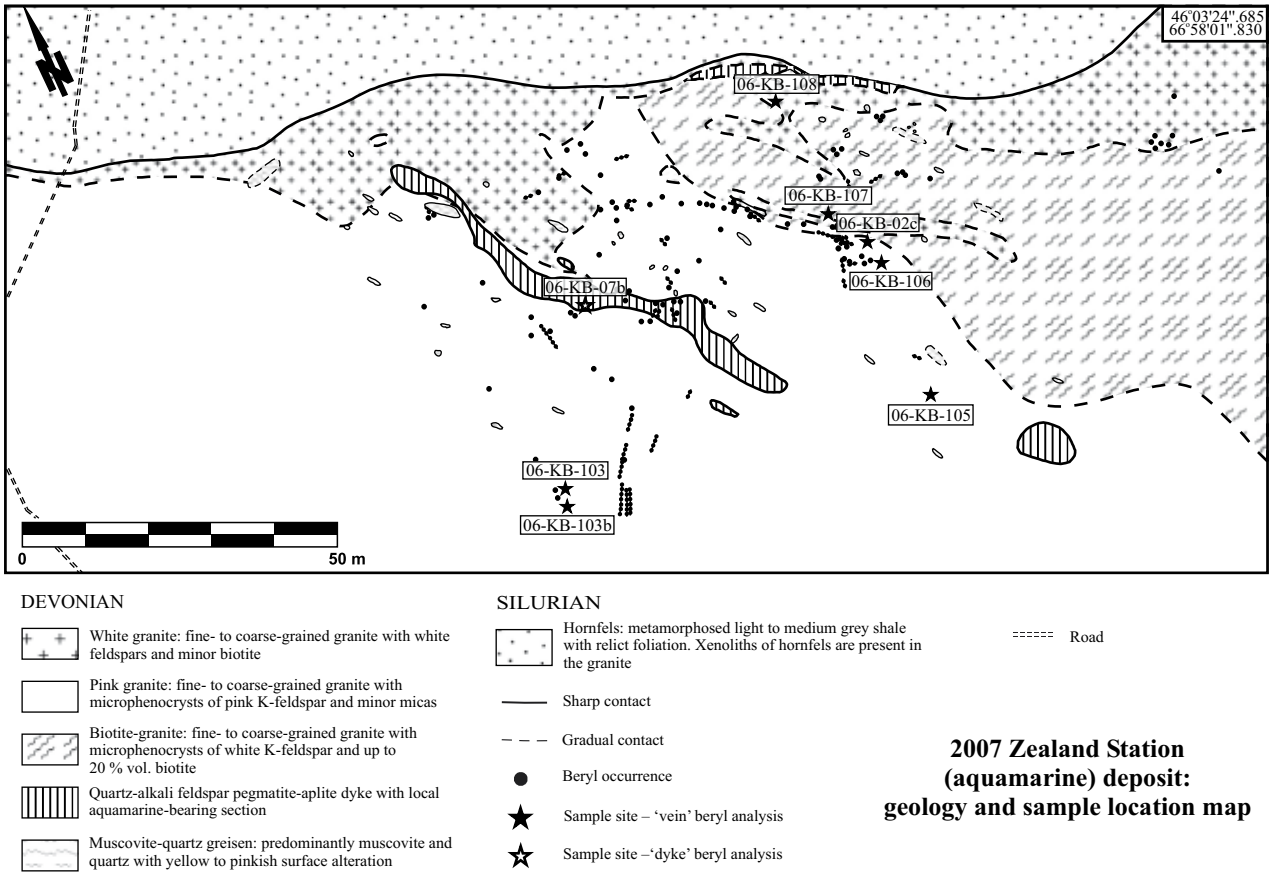

Fig. 2 Geology of the Zealand Station aquamarine occurrence (modified from Chrzanowski and Elliott 1986).

Aquamarine and molybdenite mineralization, with trace amounts of scheelite, occur locally around greisen pockets (Fig. 4) that are marked by earthy hematization on the weathered surface and moderate alteration in the surrounding host monzogranite. Muscovite grains are less than 1 mm in size and occur in clusters, whereas the quartz is very fine grained to cryptocrystalline and appears laminated. Aquamarine crystals up to 5 cm long and molybdenite booklets up to 1cm wide occur around some greisen zones.

Quartz veins contain varied amounts of quartz, feldspar, biotite, muscovite, blue aquamarine (up to 8 cm wide; Fig. 4), and molybdenite (up to 2 cm wide booklets). The veins range between 0.5 cm to rarely 10 cm wide and have two predominant orientations: 135/90° and 010/75° W (Chrzanowski and Elliott 1986).

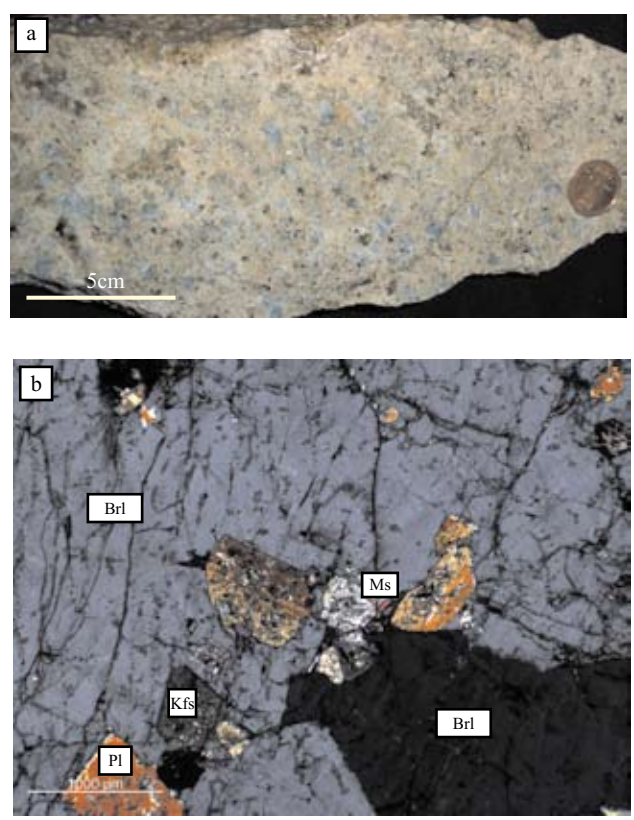

Fig. 3a – Mineralized portion of the pegmatite–aplite dyke showing 06-KB-07A. **b** – Photomicrograph in crossed polarized light depicting the relationship between magmatic beryl and surrounding minerals (06-KB-07A).

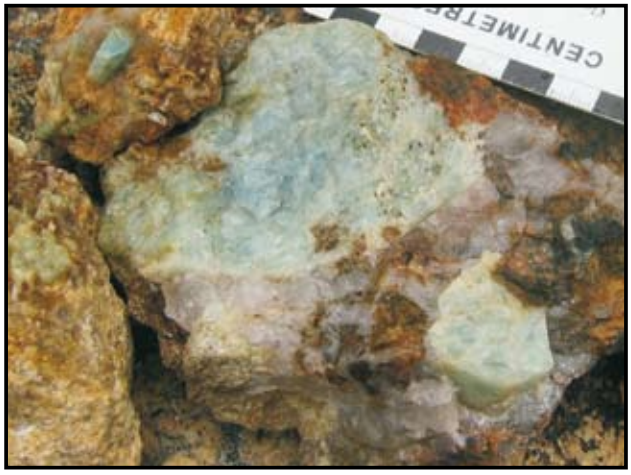

Fig. 4 Euhedral Zealand Station beryl crystals collected by a local prospector from one of the greisen veins (left) and a quartz vein (right).

3. Analytical methods

The JEOL-733 Electron Probe Microanalyser (EPMA) at the University of New Brunswick's Microscopy and Microanalysis Facility was used for the examination of aquamarine in nine large polished thin sections. The microprobe could not detect volatiles or elements lighter than boron. Operating conditions were set to a beam current of 30 nA and the data for samples were collected for 200 s (for Cs, Fe (total), Mn, Cr, V, Sc, and F), 100 s (Ca, Mg, Na, K), and 30 s (Al and Si). The following standards were used: fluorite (F), jadeite (Na), olivine (Mg), bytownite plagioclase (Al, Si, Ca), orthoclase (K), vanadium metal (V), scandium metal (Sc), chromite (Cr), bustamite (Mn), hornblende (Fe), and pollucite (Cs).

The analytical results, acquired by the EPMA, were recalculated from weight percent oxide to atoms per

Tab. 1 Average EPMA data of the zoned aquamarines from the Zealand Station

sample*	hydrothermal core average	dyke core average	hydrothermal middle average	dyke middle average	hydrothermal rim average	dyke rim average	beryl scan #1	beryl scan #6	beryl scan #12	beryl scan #18	beryl scan #24	beryl scan #31	beryl scan average
n	11	4	6	2	11	4	1	1	1	1	1	1	31
SiO_2 (*wt.%*)	67.65	67.49	67.00	67.66	67.71	67.84	67.28	66.45	66.63	66.87	66.44	67.04	66.43
Al_2O_3	17.48	16.98	17.11	16.93	17.39	17.55	17.54	17.04	17.32	17.51	17.38	17.78	17.30
Sc_2O_3	0.01	0.04	0.03	0.06	0.03	0.03	0.01	0.04	0.03	0.03	0.02	0.01	0.03
V_2O_3	0.07	0.24	0.04	0.17	0.05	0.23	0.09	0.10	0.10	0.05	0.09	0.07	0.08
Cr_2O_3	0.01	0.00	0.01	0.00	0.01	0.00	0.00	0.00	0.01	0.00	0.00	0.02	0.01
BeO*	13.62	13.59	13.40	13.52	13.54	13.72	11.50	11.35	11.39	11.43	11.37	11.43	13.77
MgO	0.42	0.54	0.39	0.51	0.39	0.38	0.49	0.47	0.44	0.32	0.39	0.24	0.40
CaO	0.01	0.00	0.01	0.01	0.01	0.01	0.00	0.00	0.00	0.00	0.01	0.00	0.00
FeO^T	0.83	1.16	1.00	1.22	0.83	0.77	0.83	1.15	0.97	0.92	1.02	0.27	0.96
Na_2O	0.33	0.46	0.39	0.40	0.32	0.34	0.34	0.32	0.31	0.25	0.28	0.17	0.30
K_2O	0.06	0.06	0.05	0.06	0.05	0.02	0.04	0.07	0.05	0.05	0.05	0.01	0.05
Cs_2O	0.03	0.09	0.07	0.10	0.08	0.06	0.03	0.10	0.10	0.07	0.09	0.04	0.08
MnO	0.01	0.00	0.01	0.00	0.00	0.01	0.01	0.01	0.00	0.01	0.00	0.00	0.01
Total	100.54	100.65	99.49	100.64	100.41	100.95	98.15	97.10	97.34	97.52	97.13	97.08	99.42
H_2O**	1.54	1.65	1.59	1.60	1.53	1.55	1.55	1.53	1.52	1.47	1.50	1.40	1.51
Si^{4+} *(apfu)****	6.040	6.040	6.047	6.050	6.048	6.035	6.026	6.032	6.026	6.029	6.021	6.043	6.027
Al^{3+}	1.840	1.790	1.821	1.784	1.831	1.840	1.852	1.823	1.846	1.861	1.857	1.889	1.850
Sc^{3+}	0.001	0.004	0.002	0.005	0.003	0.003	0.001	0.003	0.002	0.002	0.002	0.001	0.003
V^{3+}	0.005	0.017	0.003	0.012	0.003	0.017	0.006	0.007	0.007	0.004	0.007	0.005	0.006
Cr^{3+}	0.001	0.000	0.000	0.000	0.001	0.000	0.000	0.000	0.001	0.000	0.000	0.001	0.001
Mg^{2+}	0.056	0.072	0.052	0.068	0.052	0.051	0.065	0.064	0.059	0.044	0.052	0.032	0.053
Ca^{2+}	0.001	0.001	0.001	0.001	0.000	0.001	0.000	0.000	0.000	0.000	0.001	0.000	0.000
Fe^{3+}	0.048	0.068	0.052	0.079	0.049	0.045	0.062	0.087	0.073	0.070	0.077	0.021	0.072
Na^+	0.058	0.080	0.067	0.070	0.055	0.058	0.060	0.056	0.054	0.044	0.050	0.029	0.051
K^+	0.007	0.007	0.006	0.007	0.006	0.003	0.005	0.008	0.006	0.006	0.005	0.001	0.006
Cs^+	0.001	0.004	0.003	0.004	0.003	0.002	0.001	0.004	0.004	0.003	0.003	0.001	0.003
Mn^{2+}	0.000	0.000	0.001	0.001	0.000	0.001	0.000	0.000	0.000	0.001	0.000	0.000	0.000
Be^{2+}	3.000	3.000	3.000	3.000	3.000	3.000	3.000	3.000	3.000	3.000	3.000	3.000	3.000

Notes: *'dyke beryl' refers to beryl in the aquamarine-bearing section of the aplite dyke and 'hydrothermal beryl' to the beryl hosted in quartz veins and near greisenized zones.**H_2O is estimated from H_2O wt. % = (Na_2O in wt. % + 1.4829)/1.1771 (Guiliani et al. 1997). ***Compositions were recalculated on the basis of 3 Be and 18 O atoms per formula unit (apfu).

formula unit (*apfu*) with the aid of software called 'Formula' written by Dr. T.S. Ercit of the Canadian Museum of Nature (1996).

Hand-picked separates of quartz and beryl from three dyke, vein, and greisen zone samples were analyzed for oxygen isotopes; hydrogen isotopes were analyzed from the channel H_2O of beryl. Detailed analytical methods were described by Kyser et al. (1999). Estimated errors on reported ‰ values relative to V–SMOW are < 0.2 ‰ for oxygen and < 3 ‰ for hydrogen isotopes. The samples were heated to temperatures greater than 800 °C to release the channel H_2O (see Brown and Mills 1986; Fallick and Barros 1987); isotopic fractionation during the dehydration is noted to be minimal (Taylor et al. 1992).

4. Mineralogy

The aquamarine crystals at the Zealand Station deposit are clear to milky, light to medium blue in colour, commonly euhedral to subhedral, and up to 8 cm wide. There is rare zoning from dark blue in the core of the crystal to light blue in the rim seen in the aquamarine-bearing section of the dyke. The backscattered electron (BSE) images and electron microprobe study revealed simple compositional zonation in the beryl grains with euhedral to anhedral cores from both the dyke and hydrothermal sources. A total of 38 electron microprobe analyses were obtained from 12 individual beryl crystals and divided into 'dyke beryl' and 'hydrothermal beryl', the latter encompassing beryl found in both the quartz veins and greisen zones. Additional 32 analyses were obtained from one beryl crystal from a quartz vein (06-KB-108) that displayed oscillatory zonation (Table 1). The EPMA results were recalculated based on 18 O and 3 Be *apfu* giving the maximum amount of Be content and ignoring other possible substitutions in the Be-site.

Changes in the colour of beryl crystals correlate with changes in the composition (Hammarstrom 1989). The chromophores for many beryl gemstones include Cr ± V in green emerald, Mn in pink morganite, Fe^{3+} in yellow heliodor, and Fe^{2+} in blue aquamarine (Vianna et al. 2002a, b; Mihalynuk and Lett 2003), although Figueiredo et al. (2008) noted variable Fe^{3+}/Fe^{2+} in aquamarine. The measured Cr and V average concentrations were 0.0006 and 0.007 *apfu*, respectively, so the dominant chromophore is Fe. Thus the Zealand Station beryl can be classified as aquamarine.

The primary occupant of the octahedral site, Al^{3+}, contains a maximum of 2 atoms, displays a wide variation (1.745 to 1.910 *apfu*). The deficiency in the octahedral site is related to the mutual substitution of $Fe^{2+,3+}$, Mg^{2+}, Mn^{2+}, Sc^{3+}, V^{3+}, and Cr^{3+}. The expected negative trend

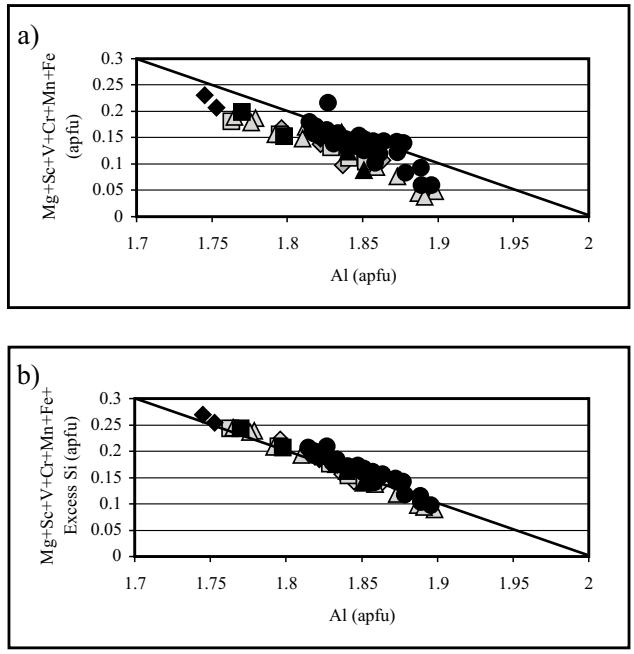

Fig. 5a – Binary plot of Al (apfu) content versus the sum of other cations in Zealand Station beryl that would substitute into the octahedral site. **b** – Al (apfu) content versus the sum of other cations plus excess Si. Symbols are scan (black circle), dyke core (black triangle), dyke middle (black square), dyke rim (black rim), hydrothermal core (grey triangle), hydrothermal rim (grey square), and hydrothermal rim (grey triangle).

from the Zealand aquamarine samples is offset below the 1:1 ratio trend by approximately 0.04 *apfu* (Fig. 5a). The Si^{4+} analyses have a maximum of 6.061 *apfu* in a tetrahedral site that permits only 6 atoms. If the excess Si is fit into the Al-bearing octahedral site as another substituting cation (Fig. 5b), the Al site is filled along the expected trend and the data show less variance.

The valency of the iron can be determined by balancing the monovalent cations (Na^+, K^+, $2Ca^{2+}$, and Cs^+) of the beryl channels with the divalent cations (Mg^{2+}, Mn^{2+}, and Fe^{2+}) of the octahedral site to a 1:1 trend. It should be noted that Ca^{2+} is included within the monovalent cations, because alkalis in the channel-sites should equal the divalent cations that substitute for Al^{3+}, but there is a charge balance deficit in the Al^{3+}-bearing site. The EPMA data from the Zealand Station aquamarine show variable right lateral offset (between 0.00 to 0.075 apfu) to the expected trend (Fig. 6a). In Fig. 6b the Fe has been removed from the divalent cations assuming the iron is in the Fe^{3+} form. The deviation is possibly due to small amounts of Fe^{2+} within the channels, but could also be due to overestimation of the monovalent cations. This assumption was also completed for aquamarine from True Blue, Yukon (Turner et al. 2007).

Alkalis, Cs, He, Ar, and water have the ability to be positioned within the beryl channels. It can be assumed

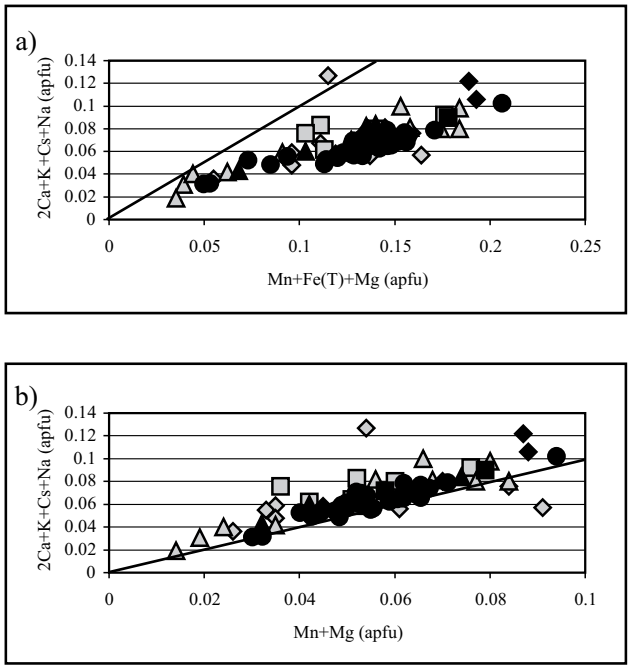

Fig. 6a – Binary plot of monovalent cations versus divalent cations in Zealand Station beryl. **b** – Monovalent cations versus divalent cations variations; all of the Fe in the Al site is assumed to be Fe^{3+}. Symbols are the same as Fig. 5.

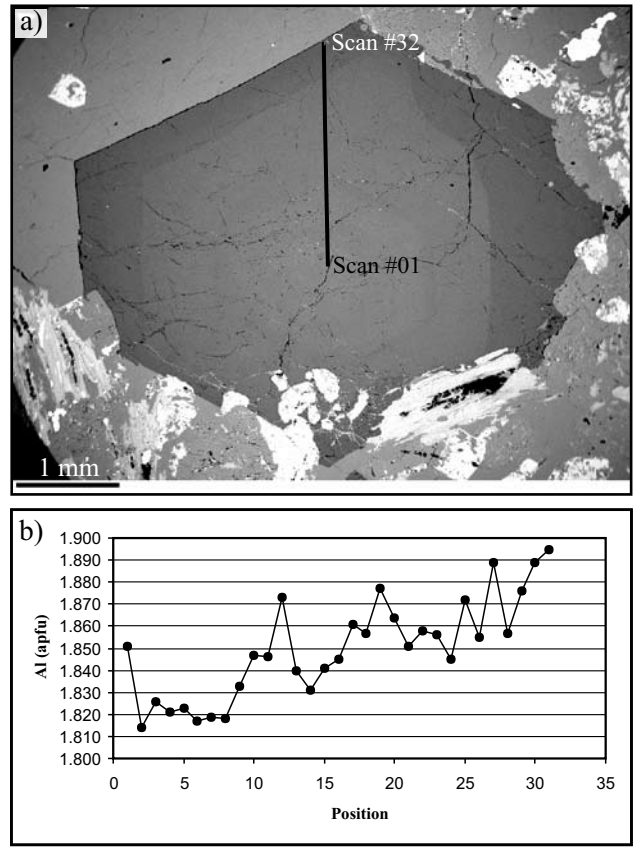

Fig. 7a – Back-scattered electron image of an aquamarine 06-KB-108 in a greisenized zone showing oscillatory zonation and the path for analyses. **b** – Al variation along the profile that is related to the substitution present in the octahedral site.

that the beryl from Zealand contains water either in the form of H_2O and/or OH. According to the empirical relationship of Giuliani et al. (1997; as defined in Brand et al. 2009), the H_2O content can be obtained from:

$$H_2O \text{ wt. \%} = (Na_2O \text{ wt. \%} + 1.4829)/1.1771.$$

Thus the average water content in the Zealand Station aquamarine samples could be calculated as 1.52 wt. %.

The hydrothermal beryl crystal that displayed oscillatory zonation is 5.5 mm in diameter and is euhedral on two sides, whereas the other sides are anhedral and in contact with sericitized plagioclase, muscovite, and quartz (Fig. 7a). The individual zones, approximately 0.1 to 0.75 mm wide, show short-range compositional variation. Many of the elements are below detection limit, but Fe^T, Mg^{2+}, Na^+, Si^{4+}, and Al^{3+} show clear variation in their concentrations. Many of these elements are associated with substitutions within the Al-bearing octahedral site (Fig. 7b). The Al content shows a general negative correlation to other elements that substitute for it, as well as Na^+ that would provide charge balance in the channels.

5. Stable isotope data

In most samples, $\delta^{18}O$ in quartz is greater than other rock-forming minerals that are more easily altered (*cf.* Taylor and Sheppard 1986), so only quartz and beryl were included in this study. As noted by Taylor et al. (1992), the H_2O released at temperatures in the excess of 800 °C (T_{REL}) is consistent with the retention of water in beryl. The molecular form of water in beryl (channel water) allows its use as a proxy for magmatic fluid isotopic composition in granites and granitic pegmatites (see synopsis in Taylor et al. 1992), mainly for the measurement of the hydrogen isotopic composition.

The $\delta^{18}O$ values of quartz are high in the pegmatite–aplite sample, but within the range for normal granites (Whalen et al. 1996); these values are comparable to the $\delta^{18}O$ of the pegmatite–aplite beryl–quartz pair analyzed (Δ 0.2 ‰). These $\delta^{18}O$ values are indistinguishable from the whole-rock values for the nearby Lake George Granodiorite (10.2 ‰), Hawkshaw Granite (9.6 ‰), and Allandale Granite (9.5 ‰) (Whalen et al. 1996; Yang et al. 2004). Whalen et al. (1996) also reported $\delta^{18}O$ values for quartz (11.9 ‰), feldspar (9.6 ‰), muscovite (8.2 ‰), and biotite (5.3 ‰) for the Allandale Granite, which are consistent with this study; these values, if in equilibrium, would reflect crystallization or quenching temperatures

to just under 500 °C (cf. Taylor et al. 1979). Such high $\delta^{18}O$ values evidently reflect derivation by contamination with an ^{18}O-enriched crustal source, typically supracrustal rocks (Longstaffe 1982; Taylor and Sheppard 1986) or specifically as a result of O isotope exchange with the wall rocks prior to final emplacement (see Taylor et al. 1979). The $\delta^{18}O$ values for the hydrothermal quartz in veins and greisens are typically higher. However, with no T estimates, the equivalent H_2O cannot be calculated, but reflect high-T metasomatism. The beryl–quartz $\delta^{18}O$ pair was analysed (Δ 1.2 ‰) from hydrothermal quartz (> 600 °C; see equation in Taylor et al. 1992).

The two δD of channel H_2O (T_{REL} > 800 °C) in beryl from the Zealand pegmatite–aplite dykes (H_2O yields of 1.3 to 1.4 wt. %) had values from –76 to –67 ‰ (Tab. 2). The δD of H_2O of channel beryl is similar to exsolved magmatic water or molecular water still dissolved in the crystallizing melt (i.e., vapour undersaturated, see Taylor 1986). However, these values are generally higher than emeralds formed at lower temperatures (<< 500 °C) (Groat et al. 2008), except for those emeralds to green beryl closely associated with pegmatite-derived fluids (see Laurs et al. 1996).

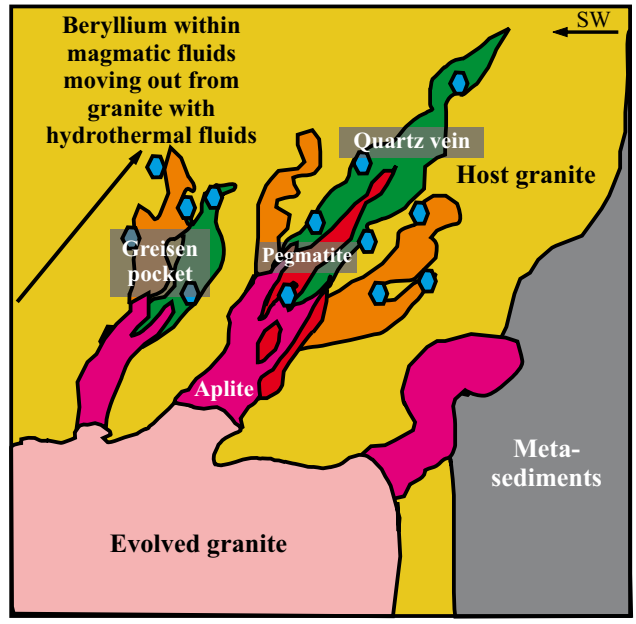

Fig. 8 Proposed genetic model for the aquamarine mineralization within the Zealand Station deposit. The blue hexagons represent beryl mineralization (modified after Groat et al. 2007).

6. Discussion

6.1. Petrogenetic aspects

The Zealand Station granitic pegmatite–aplite dykes are predominately composed of quartz, albite, and K-feldspar with minor aquamarine, muscovite, wolframite, and biotite and trace apatite, monazite, and zircon. Beal et al. (2010) concluded that the pegmatite–aplite dykes, and associated mineralization, are geochronologically and geochemically related to the Allandale Granite, the youngest and most fractionated phase of the Pokiok Batholith. The pegmatite–aplite dykes are highly fractionated compared to the parental granite, based on high incompatible elemental abundances. The dykes show characteristics typical of crustally-derived A-type granites contaminated by metasediments of the recently thickened crust as the magma was emplaced. This resulted in hybrid characteristics between NYF and LCT families of the REE pegmatite class for these dykes (Beal et al. 2010).

The heterogeneous nature of the aquamarine gem pocket in the pegmatite–aplite dyke could be explained by a late-stage exsolution of a fluid/pegmatitic phase from volatile-rich magma (Fig. 8). The water pressures would have been fairly high at their time of formation, so the aqueous pegmatitic phase coexisted with the fractionated granite (aplite) melt (Jahns and Burnham 1969). The presence of abundant beryl within one gem zone, rather than all pegmatitic zones, suggests that the fluid carry-

Tab. 2 Stable isotopic data of selected samples: δD of beryl channel H_2O content and $\delta^{18}O$ of beryl and quartz.

Sample	Source	Material	wt. % H_2O	δD(VSMOW)
06-KB-07a Beryl	Aplite Dyke	Channel water	1.4	-76
06-KB-103 Beryl	Quartz Vein	Channel water	1.3	-67
Sample		Material	Yield	$\delta^{18}O$(VSMOW)
06-KB-07a	Aplite Dyke	Beryl	15.7	10.6
06-KB-07a	Aplite Dyke	Quartz (<10% contamination)	15.6	10.4
06-KB-103	Quartz Vein	Beryl	16.1	10.2
06-KB-103	Quartz Vein	Quartz (~15% contamination)	15.7	11.4
06-KB-09a	Greisen Zone	Quartz (~15% contamination)	16.1	12.6

ing the components necessary for beryl formation was heterogeneous. The gem zone is not as fully developed as those seen on Elba Island in Italy and Mt. Mica in Maine, US, suggesting that the separate fluid phase did not evolve sufficiently to form open miariolitic cavities before crystallization (*cf.* Simmons 2007).

The aquamarine present within certain vein sets could have formed from a supercritical fluid exsolving from the magma during progressive crystallization (Candela 1997). The veins follow a joint set that has an approximate NW–SE trend but deviations exist. Greisen is related to fluids associated with the dykes in the exocontact zone of a beryllium-bearing intrusion at depth. Greisen formed presumably by a reaction of a high-temperature, siliceous magmatic fluid with elevated F concentrations. This resulted in autometasomatic alteration within the dykes and along joints at lower temperatures (~300–550 °C) crystallizing mica, feldspar, quartz–feldspar, and quartz veins (*cf.* Kievlenko 2003; Turner and Groat 2007).

6.2. Beryl systematics

The aquamarine crystals located in the dyke and hydrothermal sources show similar elemental substitutions and properties; they also indicate decreased vacancy-site substitutions in the rim compared to the core. The decreasing occupancy in the channel site is more notable in the aquamarine-rich section of the dyke as the channel substituents contents decrease continuously from 0.091 *apfu* in the core to 0.064 *apfu* in the rim; the aquamarine from hydrothermal sources decrease from 0.066 *apfu* in the core to 0.064 *apfu* in the rim. The oscillatory-zoned crystal reveals decreased vacancy-site substitution (average 0.060 *apfu*) compared to other simply-zoned aquamarine of the hydrothermal and dyke sources with a decrease from the core (0.066 *apfu*) to the rim (0.032 *apfu*). This type of channel-site zonation is common in beryl from the Bikita granitic pegmatite, Zimbabwe (Černý 2002). The aquamarine from the dyke contains increased H_2O (average 1.60 wt. %) compared to the aquamarine from hydrothermal sources (1.55 wt. %). The oscillatory-zoned aquamarine contains up to 1.66 wt. % H_2O with an average of 1.51 wt. %. According to Taylor et al. (1992), beryls from granitic pegmatites range between 1.2 and 2.55 wt. % H_2O.

The dyke-hosted aquamarine crystals also show decreased substitution in the octahedral-site as the Al-content increases from 1.79 *apfu* in the core to 1.84 *apfu* in the rim. This type of zoning is similar to that described by Abdalla and Mohamed (1999) for beryl associated with the Pan-African Belt in Egypt, but is opposite to that recorded by other authors where the zoning is explained by the exchange reaction with other minerals present (Franz et al. 1986). Additional role is played by a decrease of temperature and pressure during, or after, uplift of the dyke (Aurisicchio et al. 1988). Aquamarines from both the aquamarine-rich section of the dyke and hydrothermal sources show a greater concentration of Al in the immediate vicinity of microfractures; this type of alteration also occurs in the emeralds of Carnaiba, Bahia State, Brazil (Giuliani 1988).

The presence of excess silica is common when the Be-site (3 atoms) or Al-site (2 atoms) is assumed full to calculate the beryl formula (Sanders and Doff 1991; Abdalla and Mohamed 1999; Groat et al. 2002; Černý et al. 2003; Turner et al. 2007). Excess silica can be assigned to the Be tetrahedron (Aurisicchio et al. 1988) permitting the coupled substitution Be + 2Al = Si + 2(Fe, Mg) (Sanders and Doff 1991). The silica standard used for EPMA calibration may have caused the excess silica issue for a number of analyses with excess silica in the calculations.

Average Fe concentrations in the Zealand Station aquamarine crystals range from 0.83 to 1.22 wt. % $FeO^{T,}$ with a maximum iron content of 1.4 wt. % FeO^T that is assumed to be predominately in the Fe^{3+} state. Cores are enriched in iron relative to rims of the individual crystals. The aquamarine in the dykes contains increased average Fe (0.064 *apfu*), and V (0.015 *apfu*) compared to the aquamarine in hydrothermal sources (0.050 and 0.004 *apfu*, respectively). The iron content of the Zealand Station aquamarine is generally lower than in other reported aquamarines; the highest reported value in beryl was from dark blue aquamarine, True Blue in Yukon, Canada that contained up to 5.92 wt. % FeO^T (Turner et al. 2007).

How chromophores affect the colour of minerals, particularly beryl, is not well-understood. According to Mihalynuk and Lett (2003), Fe can occupy many sites within the structure to produce colour; Fe^{3+} within the octahedral site yields a yellow colour, while Fe^{2+} in the same site has no effect. It is the presence of Fe^{2+} within channels that produces a deep blue colour, characteristic of aquamarine gemstones (Mihalynuk and Lett 2003). Others, particularly Goldman et al. (1978) and Rossman (1981), explained that blue, green, and yellow tones are the result of different Fe^{2+}/Fe^{3+} ratios (see Černý 2002). Another suggestion is that intervalence charge transfer (IVTC) occurs between Fe^{2+} and Fe^{3+}, whereby the Fe^{2+} is located at the Al sites and the Fe^{3+} is located at an interstitial octahedral position that lies between the Al-sites and is normally empty. It is well documented that the long-term exposure of beryl to light and associated radiation will cause colour fading, because of IVTC (Samoilovich et al. 1971; Nassau 1978; Mathew et al. 2000; Groat et al. 2005).

The aquamarine at the Zealand Station, with an empirically derived average water content of 1.52 wt. %, crystallized between 600 and 660 °C at 2.5 ± 0.5 kbar (200–300

MPa) according to experimental constraints provided by Pankrath and Langer (2002). This is consistent with the H_2O yield (1.3 and 1.4 wt. %) from the two H isotope analyses of channel beryl and with a modified liquidus and solidus relations in extremely fractionated pegmatite during hypabyssal emplacement (see London 2005).

7. Conclusions

The Zealand Station deposit contains locally abundant beryl mineralization; there are also variable amounts of molybdenite, wolframite, and scheelite. The beryl samples collected all have microfractures, although the presence of gem-quality beryl samples is possible beneath the zone of deep weathering. Wolframite and scheelite mineralization is present locally, although molybdenite is rather abundant within the magmatically-derived quartz veins and around greisen pockets in the granitic host rock.

Other highlighted conclusions from the Zealand Station aquamarine occurrence:

1. The electron-microprobe analyses of Zealand Station aquamarine in both dykes and veins revealed that the main chromophore is Fe^{3+} within the Al-bearing site with a maximum of 1.4 wt. % FeO^T present. This justifies the use of the term 'aquamarine' to describe this beryl. Zonation was visible in all crystals in the BSE image.
2. The aquamarine crystals contain more silica than the Si-bearing tetrahedral site permits; the excess silica fits perfectly as a substituent for Al within in the Al-bearing octahedral site; however, this is likely a result of the silica standard used to calibrate the EPMA. It is recommended to introduce a new beryl standard with known silica content so the common issue of excess silica could be properly addressed.
3. Additional geochemical features of the aquamarine crystals include increased octahedral-site substitutions from the core to the rim in the magmatic aquamarine and increased channel-site substitutions from the core to rim in both the magmatic and hydrothermal aquamarine.
4. The average water content was calculated based on the equation H_2O wt. % = (Na_2O wt. % + 1.4829)/1.1771 at 1.53 wt. %, similar to the yields of 1.3 and 1.4 wt. % for the channel water.
5. The high $\delta^{18}O$ values for quartz and beryl are consistent with a considerable crustal component to the magmas and the lower δD values of the channel water in beryl reflect crystallization from a volatile-undersaturated magmatic source before dyke emplacement.

Acknowledgements The valuable suggestions and constructive comments on a previous version of this manuscript by Drs. Steve R. McCutcheon and Kathleen Thorne are appreciated. We are very grateful to Prof. Lee Groat (UBC) for his guidance in beryl analyses and structure interpretations, and Dr. Doug Hall helped with EPMA and SEM imaging at UNB. A special thank you is extended to L. Lawrence for giving me access to the property and helping with cleaning the outcrops. We thank Dr. Jane Hammarstrom and Prof. Milan Novák for constructive reviews and suggestions. Funding for this project was provided by the Department of Natural Resources – Minerals Division and a Natural Sciences and Engineering Research Council of Canada – Discovery Grant to David Lentz.

References

Aurisicchio C, Fioravanti G, Grubessi O, Zanazzi PF (1988) Reappraisal of the crystal chemistry of beryl. Amer Miner 73: 826–837

Abdalla HM, Mohamed FH (1999) Mineralogical and geochemical investigation of emerald and beryl mineralization, Pan-African Belt of Egypt: genetic and exploration aspects. J Afr Earth Sci 28: 581–598

Beal K, Lentz DR, Hall D, Dunning G (2010) Mineralogical, geochronological, and geochemical characterization of the Early Devonian aquamarine-bearing dykes of the Zealand Station Be–Mo deposit, west-central NB. Can J Earth Sci 47: in press

Brand AA, Groat LA, Linnen RL, Garland MI, Breaks FW, Giuliani G (2009) Emerald mineralization associated with the Mavis Lake pegmatite group, near Dryden, Ontario. Canad Mineral 47: 315–336

Brown Jr. GE, Mills BA (1986) High-temperature structure and crystal chemistry of hydrous alkali-rich beryl from the Harding pegmatite, Taos County, New Mexico. Amer Miner 71: 547–556

Candela PA (1997) A review of shallow, ore-related granites: textures, volatiles, and ore metals. J Petrol 38: 1619–1633

Caron A (1996) Geology of the Pokiok Batholith aureole, with emphasis on the Lake George Mine, York County, New Brunswick. Natural Resources and Energy, Geoscience Report 94-2: 1–91

Chrzanowski MJ, Elliott CG (1986) Progress report beryllium Zealand Station, N.B. (21J/02). New Brunswick Department of Natural Resources Division, Open File 473350, pp 1–18

Černý P (2002) Mineralogy of beryllium in granitic pegmatites. In: Grew ES (ed) Beryllium – Mineralogy, Petrology and Geochemistry. Rev Mineral Geochem 50: 405–444

Černý P, Anderson AJ, Tomascak PB, Chapman R (2003) Geochemical and morphological features of beryl from

the Bikita granitic pegmatite, Zimbabwe. Canad Mineral 41: 1003–1011

Diego Gatta G, Nestola F, Bromiley GD, Mattauch S (2006) The real topological configuration of the extra-framework content in alkali-poor beryl: a multi-methodological study. Amer Miner 91: 29–34

Fallick AE, Barros JG (1987) A stable-isotope investigation into the origin of beryl and emerald from the Porangatu deposits, Goias State, Brazil. Chem Geol (Isot Geosci Sect) 66: 293–300

Figueiredo MO, Pereira da Silva T, Veiga JP, Leal Gomes C, De Andrade V (2008) The blue colouring of beryls from Licungo, Mozambique: an X-ray absorption spectroscopy study at the iron K-edge. Mineral Mag 72: 175–178

Franz G, Grundmann G, Ackermand D (1986) Rock-forming beryl from a regional metamorphic terrain (Tauern Window, Austria). Tschermaks mineral petrogr Mitt 35: 167–192

Giuliani G (1988) Scanning electron microscopy (SEM) and its applications: determination of solid daughter minerals in fluid inclusions. Congresso Latino-Americano de Geologia 7: 445–458

Giuliani G, France-Lanord C, Zimmermann JL, Cheil-Letz A, Arboleda C, Charoy B, Coget P, Fontan F, Giard D (1997) Fluid composition, δD of channel H_2O, and $\delta^{18}O$ of lattice oxygen in beryls: genetic implications for Brazilian, Colombian, and Afghanistani emerald deposits. Int Geol Rev 39: 400–424

Goldman DS, Rossman GR, Parkin KM (1978) Channel constituents in beryl. Phys Chem Miner 3: 225–235

Grew ES (2002) Mineralogy, petrology, and geochemistry of beryllium: an introduction and list of beryllium minerals. In: Grew ES (ed) Beryllium – Mineralogy, Petrology and Geochemistry. Rev Mineral Geochem 50: 1–76

Groat LA, Marshall DD, Giuliani G, Murphy DC, Piercey SJ, Lambor JL, Mortensen JK, Ercit TS, Gault RA, Mattey DP, Schwarz D, Maluski H, Wise MA, Wengzynowski W, Eaton DW (2002) Mineralogical and geochemical study of the Regal Ridge emerald showing, southeastern Yukon. Canad Mineral 40: 1313–1338

Groat LA, Hart CJR, Lewis LL, Neufeld HLD (2005) Emerald and aquamarine mineralization in Canada. Geosci Can 32: 65–76

Groat LA, Giuliani G, Marshall DD, Turner D (2007) Emerald. In: Groat LA (ed) Geology of Gem Deposits. Mineralogical Association of Canada 37: 79–100.

Groat LA, Giuliani G, Marshal DD, Turner D (2008) Emerald deposits and occurrences: a review. Ore Geol Rev 34: 87–112

Hammarstrom JM (1989) Mineral chemistry of emeralds and some associated minerals from Pakistan and Afghanistan: an electron microprobe study. In: Kazmi AH, Snee LW (eds) Emeralds of Pakistan: Geology, Gemology, and Genesis. Geological Survey of Pakistan and Van Nostrand Reinhold Co. Inc., New York, pp 125–150

Hawthorne FC, Huminicki DMC (2002) The crystal chemistry of beryllium. In: Grew ES (ed) Beryllium – Mineralogy, Petrology and Geochemistry. Rev Mineral Geochem 50: 333–404

Jahns RH, Burnham CW (1969) Experimental studies of pegmatite genesis; I, A model for the derivation and crystallization of granitic pegmatites. Econ Geol 64: 843–864

Kievlenko EY (2003) Beryl. In: Soregaroli A (ed) Geology of Gems. Ocean Pictures Ltd., Colorado, pp 71–119

Kyser TK, O'Hanley DS, Wicks FJ (1999) The origin of fluids associated with serpentinization processes: evidence from stable-isotope compositions. Canad Mineral 37: 223–237

Laurs BM, Dilles JH, Snee LW (1996) Emerald mineralization and metasomatism of amphibolite, Khaltaro granitic pegmatite hydrothermal vein system, Haramosh Mountains, northern Pakistan. Canad Mineral 34: 1253–1286

London D (2005) Granitic pegmatites: an assessment of current concepts and directions for the future. Lithos 80: 281–303

Longstaffe FJ (1982) Stable-isotopes in the study of granitic pegmatites and related rocks. In: Černý P (ed) Granitic Pegmatites in Science and Industry. Mineral Association of Canada, Short Course 8: 373–404

Mathew G, Karanth RV, Gundu Rao RK, Deshpande RS (2000) Colouration in natural beryls: a spectroscopic investigation. J Geol Soc India 56: 285–303

Mihalynuk MG, Lett R (2003) Composition of Logtung beryl (aquamarine) by ICPES/MS: a comparison of beryl worldwide. In: Geological Fieldwork 2003. Crown Publications Inc., British Columbia, pp 141–146

Nassau K (1978) The origins of color in minerals. Amer Miner 63: 219–229

Pankrath R, Langer K (2002) Molecular water in beryl, $^{VI}Al_2[Be_3Si_6O_{18}]\cdot nH_2O$, as a function of pressure and temperature: an experimental study. Amer Miner 87: 238–244

Rast DC, Skehan JW (1993) Mid-Paleozoic orogenesis in the North Atlantic: the Acadian Orogeny. In: Roy DC, Skehan JW (eds) The Acadian Orogeny: Recent Studies in New England, Maritime Canada, and the Autochthonous Foreland. Geol Soc Spec Papers 275: 1–26

Rossman GR (1981) Origin of color in pegmatite minerals. In: Brown GE (ed) The Mineralogy of Pegmatites. Mineralogical Society of America – Friends of Mineralogy Symposium, Tuscon, Arizona, pp 1–6

Samoilovich MI, Tsinober LI, Dunin-Barkovskii RL (1971) Nature of the coloring in iron-containing beryl. Sov Phys – Crystallography 16: 147–150

Sanders IS, Doff DH (1991) A blue sodic beryl from southeast Ireland. Mineral Mag 55: 167–172

Simmons WB (2007) Gem-bearing pegmatites. In: Groat LA (ed) Geology of Gem Deposits. Mineralogical Association of Canada 37: 169–206

Taylor BE (1986) Magmatic volatiles: isotopic variation of C, H, and S. In: Valley JW, Taylor HP Jr, O'Neil JR (eds) Stable Isotopes in High Temperature Geological Processes. Mineral Soc Am Rev Mineral 16: 185–225

Taylor BE, Foord EE, Friedrichsen HE (1979) Stable isotope and fluid inclusion studies of gem-bearing granitic pegmatite–aplite dikes, San Diego Co., California. Contrib Mineral Petrol 68: 187–205

Taylor HP Jr, Sheppard SMF (1986) Igneous rocks: I. Processes of isotopic fractionation and isotopic systematics. In: Valley JW, Taylor HP Jr, O'Neil JR (eds) Stable Isotopes in High Temperature Geological Processes. Mineral Soc Am Rev Mineral 16: 227–271

Taylor RP, Fallick AE, Breaks FW (1992) Volatile evolution in Archean rare element granitic pegmatites: evidence from the hydrogen isotopic composition of channel H_2O in beryl. Canad Mineral 30: 877–893

Turner D, Groat LA (2007) Non-emerald gem beryl. In: Groat LA (ed) Geology of Gem Deposits. Mineralogical Association of Canada 37: 111–143

Turner D, Groat LE, Hart CJR, Mortensen JK, Linnen RL, Giuliani G, Wengzynowski W (2007) Mineralogical and geochemical study of the True Blue aquamarine showing, southern Yukon. Canad Mineral 45: 203–227

Vianna P, da Costa G, Grave E, Evangelista H, Stern W (2002a) Characterization of beryl (aquamarine variety) by Mössbauer spectroscopy. Phys Chem Miner 29: 78–86

Vianna R, Jordt-Evangelista H, da Costa G, Stern W (2002b) Characterization of beryl (aquamarine variety) from pegmatites of Minas Gerais, Brazil. Phys Chem Miner 29: 668–679

Wang RC, Che XD, Zhang WL, Zhang AC, Zhang H (2009) Geochemical evolution and late re-equilibrium of Na-Cs-rich beryl from the Koktokay #3 pegmatite (Altai, NW China). Eur J Mineral 21: 795–809

Whalen JB (1993) Geology, petrography, and geochemistry of Appalachian granites in New Brunswick and Gaspésie, Quebec. Geol Surv Canad Bull 436: 1–124

Whalen JB, Jenner GA, Longstaffe FJ, Hegner E (1996) Nature and evolution of the eastern margin of Iapetus: geochemical and isotopic constraints from Siluro–Devonian granitoid plutons in the New Brunswick Appalachians. Can J Earth Sci 33: 140–155

Yang XM, Lentz DR, Chi G, Kyser K (2004) Fluid–mineral reaction in the Lake George Granodiorite, New Brunswick, Canada: implications for Au–W–Mo–Sb mineralization. Canad Mineral 42: 1443–1464